



저작자표시-비영리-변경금지 2.0 대한민국

이용자는 아래의 조건을 따르는 경우에 한하여 자유롭게

- 이 저작물을 복제, 배포, 전송, 전시, 공연 및 방송할 수 있습니다.

다음과 같은 조건을 따라야 합니다:



저작자표시. 귀하는 원저작자를 표시하여야 합니다.



비영리. 귀하는 이 저작물을 영리 목적으로 이용할 수 없습니다.



변경금지. 귀하는 이 저작물을 개작, 변형 또는 가공할 수 없습니다.

- 귀하는, 이 저작물의 재이용이나 배포의 경우, 이 저작물에 적용된 이용허락조건을 명확하게 나타내어야 합니다.
- 저작권자로부터 별도의 허가를 받으면 이러한 조건들은 적용되지 않습니다.

저작권법에 따른 이용자의 권리는 위의 내용에 의하여 영향을 받지 않습니다.

이것은 [이용허락규약\(Legal Code\)](#)을 이해하기 쉽게 요약한 것입니다.

[Disclaimer](#)

Master's Thesis

# Surface Functionalization for a High-Performance Lithium Metal Anode

Ukhyun Jung

School of Energy and Chemical Engineering  
Energy Engineering(Battery Science and Engineering)

Ulsan National Institute of Science and Technology

2022

# Surface Functionalization for a High-Performance Lithium Metal Anode

Ukhyun Jung

School of Energy and Chemical Engineering  
Energy Engineering(Battery Science and Engineering)

Ulsan National Institute of Science and Technology

# Surface Functionalization for a High-Performance Lithium Metal Anode

A thesis/dissertation submitted to  
Ulsan National Institute of Science and Technology  
in partial fulfillment of the  
requirements for the degree of  
Master of Science

Ukhyun Jung

12.08.2021 of submission

Approved by



---

Advisor

Hyun-Wook Lee

# Surface Functionalization for a High-Performance Lithium Metal Anode

Ukhyun Jung

This certifies that the thesis/dissertation of Ukhyun Jung is approved.

12.08.2021 of submission

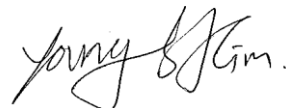
Signature



---

Advisor: Hyun-Wook Lee

Signature



---

Youngsik Kim

Signature



---

Sung-Kyun Jung

Signature

## Abstract

Lithium-ion batteries (LIB) have been the backbone of the success of numerous electronics in our everyday lives. Nonetheless, the development of large-scale Energy Storage Systems (ESS) and Electric Vehicles (EV) now require battery systems with capacities that far surpass the current lithium-ion batteries. Lithium metal batteries (LMB) have been actively researched thanks to the lithium metal that is used as their anode. The lithium metal anode is considered as the ‘holy grail’ of anode materials due to its low density ( $0.54 \text{ g/cm}^3$ ), low redox potential ( $-3.04 \text{ V vs SHE}$ ), and its high specific capacity ( $3860 \text{ mAh/g}$ ).

However, the severe performance degradation due to the intrinsic characteristics of lithium metal prevents it from being utilized as a battery material despite its excellent properties. A great deal of the research aiming for a practical lithium metal anode targets the electrolyte yet does not consider how this would affect the cathode. Herein, an electrode of which its surface is modified using thermal treatment with silica ( $\text{SiO}_2$ ) and silicon nitride ( $\text{Si}_3\text{N}_4$ ) as to negate performance damaging phenomenon and having no change to the electrolyte is proposed. The lithium metal anode modification is confined to the surface of the electrode thus having minimum influence on the cathode. Electrode surface characterization is carried out by SEM observation and XPS analysis revealing the SEI layer structure. Electrochemical performance evaluated using symmetrical cells reveal that modified electrodes show a significantly lower overpotential for over 1000 cycles at a current density of  $1 \text{ mA/cm}^2$ . Kinetic properties were also evaluated through Tafel plots and the activation energies of each electrode. Full cell (NCM622 cathode) electrochemical evaluation reveals a capacity retention of over 75% at 700 cycles, and an extremely high coulombic efficiency over 99.9% for the modified electrodes. Operando optical microscope observation of lithium plating on the surface of each electrode is also conducted to further confirm the modification’s effect on the property of the electrode. Overall, the modified electrodes show significantly enhanced performance and surface properties. This work proposes a simple method to produce surface modified lithium metal anodes based on thermal treatment for practical lithium metal batteries.



## Contents

<b>Abstract</b> -----	5
<b>List of Figures</b> -----	8
<b>1. Research Background</b> -----	9
1.1 Lithium-ion batteries-----	9
1.2 Lithium metal anodes-----	10
<b>2. The Surface Functionalization of Lithium Metal Anodes</b> -----	15
2.1 Experimental-----	15
2.2 Results and Discussion-----	18
2.3 Conclusion-----	28
<b>3. References</b> -----	29



## List of figures

**Figure 1.** The growth of the market for lithium-ion batteries in the U.S. up until 2027

**Figure 2.** The high energy density of lithium metal anodes and the prominent drawbacks of using a lithium metal anode.

**Figure 3.** The cyclability reduction of cells at elevated temperatures when FEC additive exists in the electrolyte system.

**Figure 4.** Lithium metal anodes modified in the form of lithium metal alloy with silicon ( $\text{Li}_x\text{Si}_y$ )

**Figure 5.** Lithium metal anodes modified with lithium metal alloy w/ functional groups. The modification is confined to the surface of the electrode.

**Figure 6.** Scattering electron microscope (SEM) images of the electrode's surfaces after modification

**Figure 7.** X-ray photoelectron spectroscopy (XPS) spectrum of each electrode right after their modifications.

**Figure 8.** XPS depth profiling of the surfaces of each electrode after SEI layer formation.

**Figure 9.** Cycling tests of symmetrical cells using modified lithium metal anodes vs a bare lithium metal anode.

**Figure 10.** Overpotential profiles for current tests running in 10 cycles each at changing current densities from 1 mA/cm<sup>2</sup>, 3 mA/cm<sup>2</sup>, 5 mA/cm<sup>2</sup>, and back to 1 mA/cm<sup>2</sup>

**Figure 11.** Tafel plots (left) and activation energies (right) of the modified electrodes.

**Figure 12.** Full cell electrochemical performance. a) Initial capacity shown through a formation cycle. b) Cycle retention and coulombic efficiency (CE) of full cells using modified lithium metal anodes and NCM622 cathode.

**Figure 13.** Lithium plating observed through operando OM observation. a-d. Lithium plating observed on the surface of each modified electrode. e. Lithium deposition thickness mapped by time and f. the density of the lithium plated throughout the surface of each electrode.

## Research Background

### 1.1 Lithium-ion Batteries

Ever since the lithium-ion battery has been commercialized, they have shown an immense amount of influence in our everyday lives. However, electric vehicles, large-scale energy storage systems, and other future applications demands the performance of which the current lithium-ion battery simply cannot supply. The intrinsic capacity limitation of the commercialized lithium-ion battery prevents it from being used in future applications.

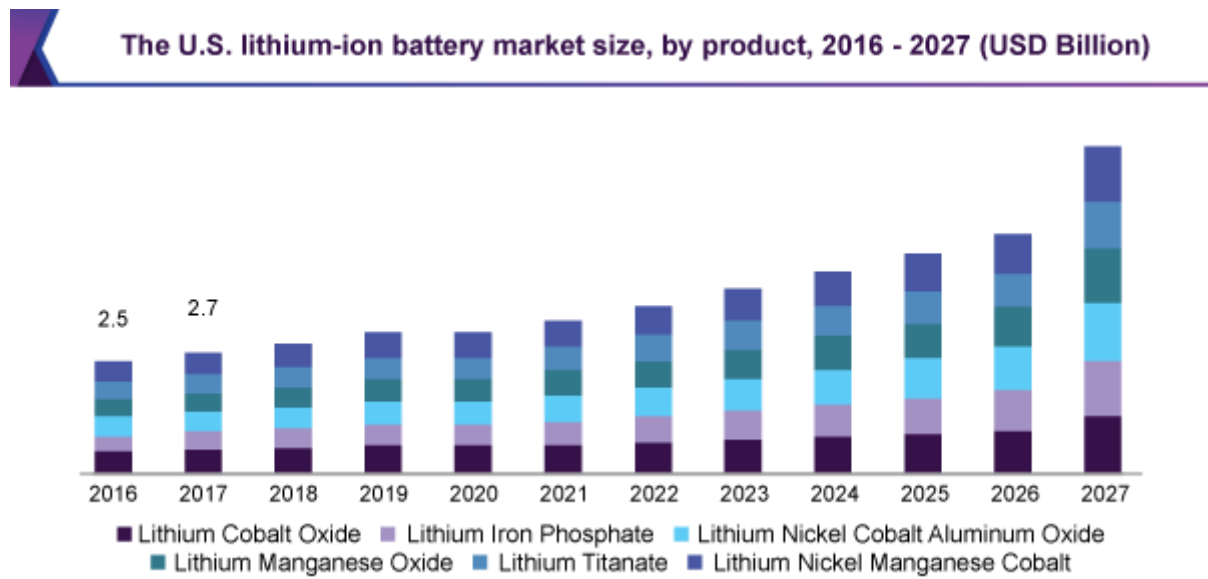


Figure 1. The growth of the market for lithium-ion batteries in the U.S. up until 2027.

## 1.2 Lithium Metal Anodes

Various research is on-going for the demand of high-capacity batteries, one of them being the lithium metal anode. Using lithium metal as the anode seems to be almost common sense, when considering its properties. Its high specific capacity (3,860 mAh/cm<sup>2</sup>) and low reduction potential (-3.04 vs SHE) makes it one of the most desirable anode materials <sup>1,2</sup>. Lithium metal batteries have been actively researched due to these properties.

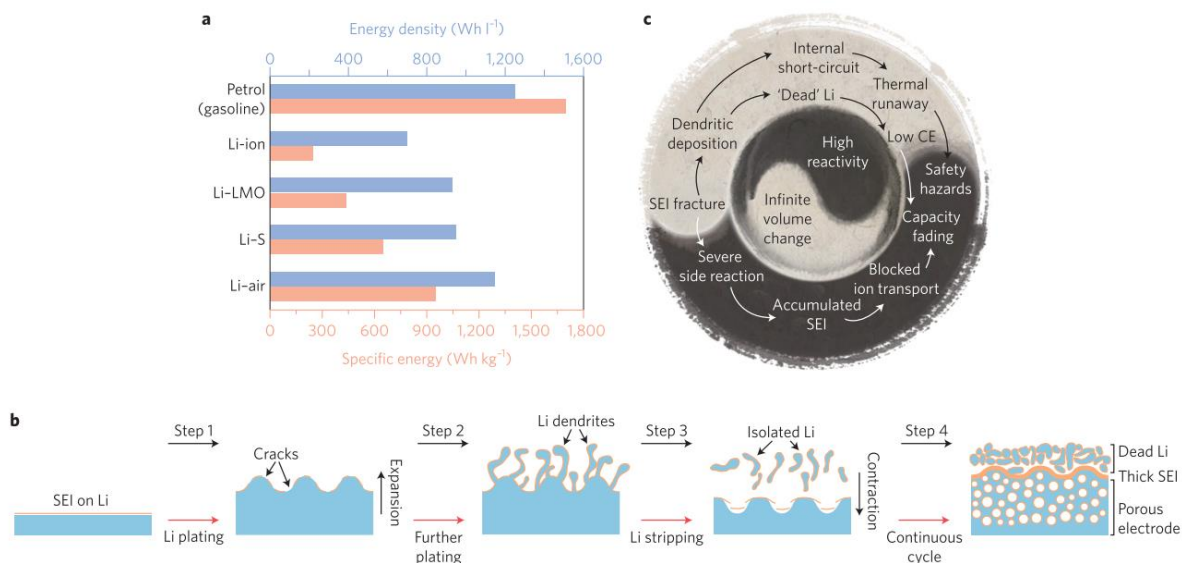


Figure 2. The high energy density of lithium metal anodes and the prominent drawbacks of using a lithium metal anode.

However, despite these positive traits, lithium metal anodes are not even near practical use because of its distinct weaknesses <sup>3,4</sup>. When lithium ions go through nucleation on the lithium metal surface, following lithium ions tend to concentrate on the newly formed lithium metal seed causing dramatic, needle-like dendrite growth which acts as a safety hazard when it punctures through the separator and reaches the cathode leading to possible explosion of the battery <sup>2</sup>. This potential explosion issue is not the only major problem lithium metal anodes have. Due to its lack of a host for lithium deposition, lithium is plated directly on the surface of the electrode causing relatively infinite volume change. During the cycling of the electrode, its volume change causes the solid electrolyte interface to crack and when this happens repeatedly, the SEI layer thickens and become inefficient in terms of ionic conductivity <sup>5</sup>. During this process electrolyte consumption is accelerated, which shortens the battery's life significantly. Also, during the repeated forming and breaking of the SEI layer, lithium metal is detached from the electrode surface and becomes unusable ('dead lithium') causing capacity degradation <sup>2</sup>.

There could be several approaches to solving these problems. One of the most common ways is to strengthen the SEI layer so that it can withstand the dendrite growth and volume change<sup>6-8</sup>. Another approach would be to prevent the forming of lithium dendrites on a more fundamental level. If we can distribute the lithium ionic flux uniformly on the surface of the lithium metal anode, it would minimize dendrite formation and volume change of the electrode<sup>9,10</sup>. Whichever solution is plausible through modifying the interphase layer between the electrode surface and electrolyte. Including inorganic components to form a lithium fluoride, lithium oxide rich SEI layer has proven to be more mechanically robust<sup>5,11</sup>. Uniform lithium plating requires a surface that has a high conductivity for lithium ions. Among substances that show such properties, lithium nitride has proven to be a good component for a SEI layer due to its high lithium ionic conductivity ( $1-2 * 10^{-3} \Omega^{-1} \text{ cm}^{-1}$ )<sup>12,13</sup>. A common way to produce a layer with lithium nitride is by adding lithium nitrate ( $\text{LiNO}_3$ ) additives to the electrolyte<sup>14,15</sup>. However, the usage of lithium nitrate as an additive in certain electrolytes is hindered due to its low solubility<sup>16</sup>. To overcome this obstacle, researchers are forced to perform additional steps in order to dissolve an adequate amount of lithium nitrate in carbonate electrolytes or to use an electrolyte based on ether despite its poor oxidation capability preventing it from being used in high voltage batteries (limited potential window of up to 3~4V). Both of the above solutions involve modifying the electrolyte for the benefit of the lithium metal anode.

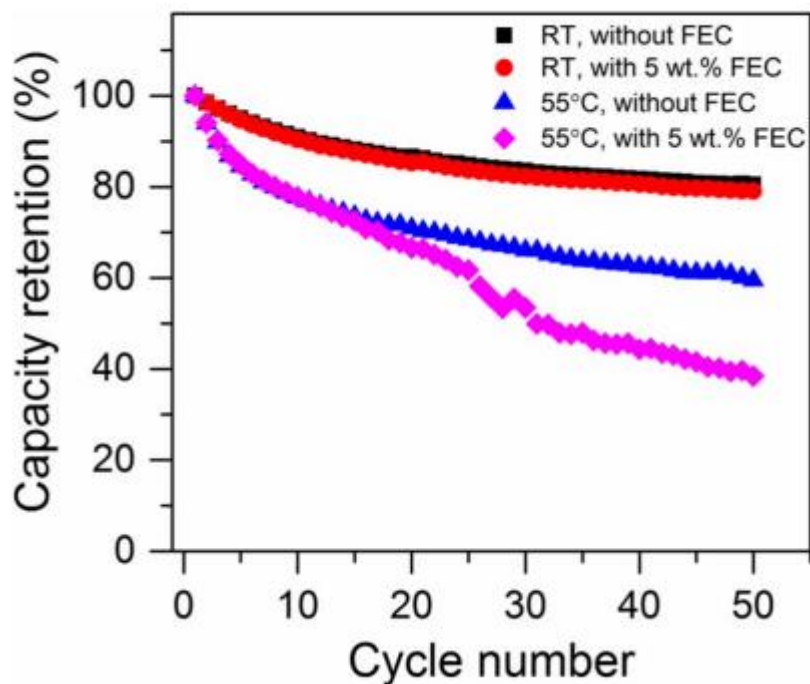


Figure 3. The cyclability reduction of cells at elevated temperatures when FEC additive exists in the electrolyte system.

However, there are cases where the electrolyte causes the cathode to have performance issues. Hosop Shin et al. reports poor cycle retention and a sharp rise in interfacial resistance at the cathode due to the dehydrofluorination of FEC additives at elevated temperatures<sup>17</sup>. Jordi Cabana et al. also illustrates the degradation of cathode material involving the dissolution of transition metal due to HF originating from electrolyte components<sup>18</sup>. As shown in the above cases, considering the possible consequences of altering the electrolyte, the authors would like to propose a lithium metal anode of which its modification is confined to the surface of the anode.

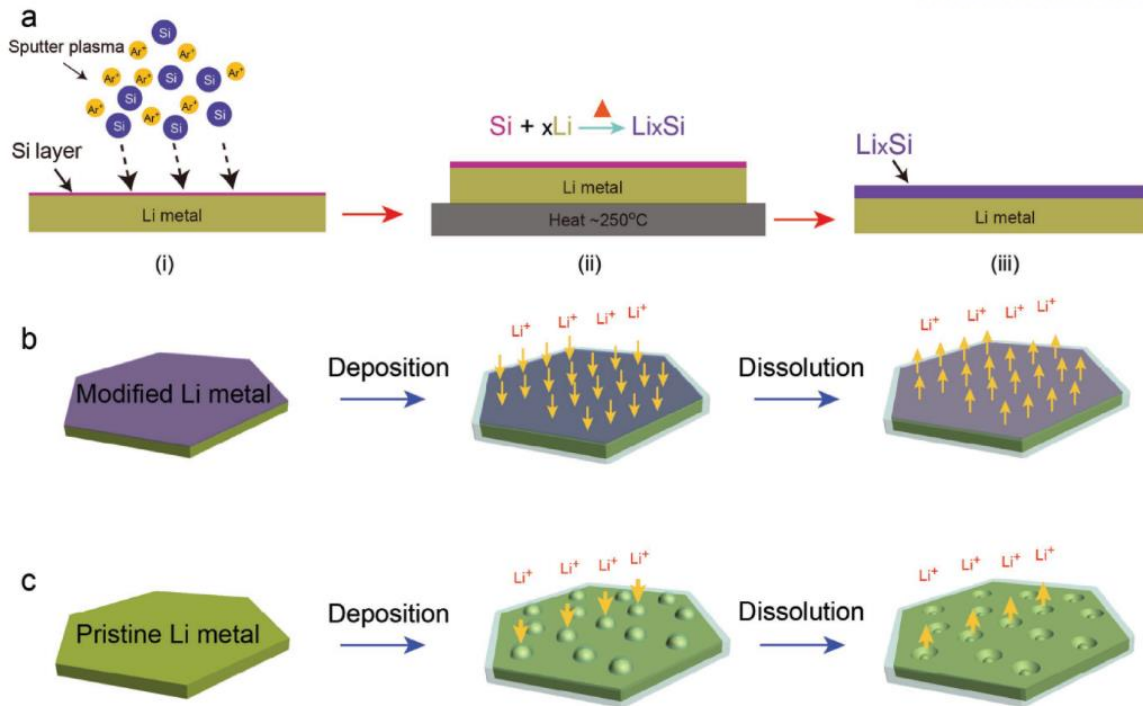


Figure 4. Lithium metal anodes modified in the form of lithium metal alloy with silicon ( $\text{Li}_x\text{Si}_y$ ).

The question remains specifically how to modify the electrode. Lithium metal alloys with functional groups would be a reasonable choice considering that lithium metal alloys have proven to help the uniform distribution of lithium-ion flux<sup>19–22</sup> and it would provide a much simpler engineering process (powder form dispersed in liquid and applied to the surface under thermal treatment). Among the many lithium metal alloys, silicon with functional groups would be a reasonable choice cost-wise ( $\text{SiO}_2$ ,  $\text{Si}_3\text{N}_4$ ). If we are going to use thermal annealing with lithium metal alloys for the surface modification, we also need a fundamental structure (scaffold) to keep the lithium metal together while the reaction is in process. For this we implemented a carbon fiber that has been shown to act as a good lithium metal host once it undergoes thermal treatment<sup>23</sup>.

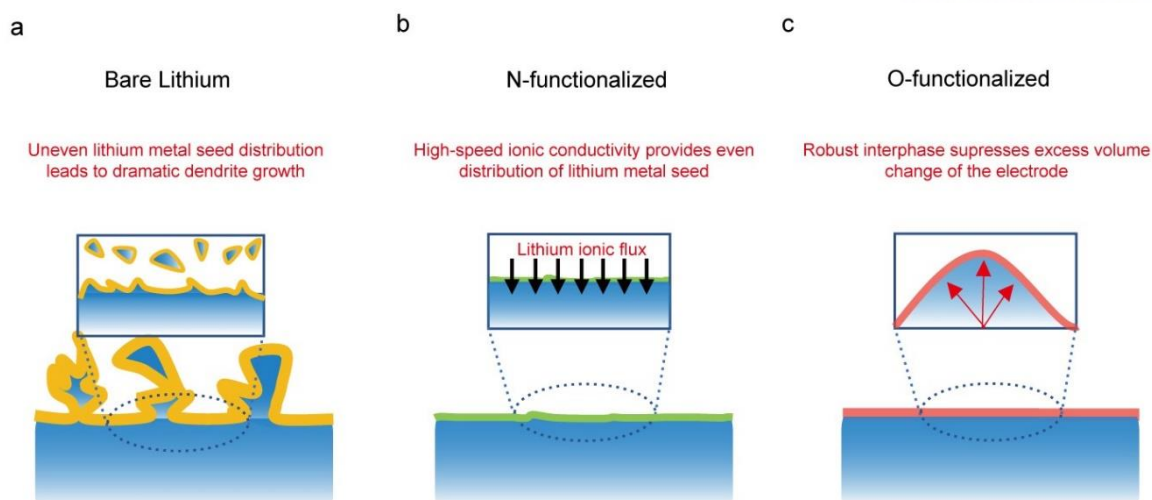


Figure 5. Lithium metal anodes modified with lithium metal alloy w/ functional groups. The modification is confined to the surface of the electrode.

Herein, we propose a lithium metal anode/carbon composite with a lithium metal alloy surface with functional groups ( $\text{SiO}_2$ ,  $\text{Si}_3\text{N}_4$ ) that shows the functionalities of a modified SEI layer. Fig 5a~c shows the schematic of the resulting electrode and the expected functionalities. This way of modifying the surface of the anode minimizes the amount of the influence towards the cathode and does not require any major changes to the electrolyte. For this reason, one of the most common electrolytes, carbonate electrolyte is used for this paper. For comparison, a lithium metal anode with no modification whatsoever, and another lithium metal anode using silicon were fabricated.

The fabricated electrodes were characterized and electrochemically evaluated thoroughly, test results implying that the existence of functional groups along with lithium metal alloy can show a significant enhancement in performance. We also observed through operando optical microscopy, that the addition of functional groups to lithium metal alloy can lead to a thinner and more even lithium deposition of the lithium metal anode surface.

## The Surface Functionalization of Lithium Metal Anodes

### 2.1 Experimental

#### Sample preparation

The modified electrodes were made in the following order. Annealed carbon cloth was used as the carbon host for lithium metal. Thermal treatment of the carbon cloth was carried out at 500 °C for 3h. It was then transferred into a glovebox to be infused with molten lithium. After the infusion process was completed, the lithium-carbon composite is laid on a stainless still pot to cool down to room temperature. A thin layer of either Si, SiO<sub>2</sub>, or Si<sub>3</sub>N<sub>4</sub> particles dispersed in dimethyl carbonate was applied onto the surface of lithium-carbon composites. The electrode was then transferred to a hot plate and heated at 300 °C for 3h to diffuse the alloying samples. The prepared surface-modified electrodes were cut by a punching tool for electrochemical characterization.



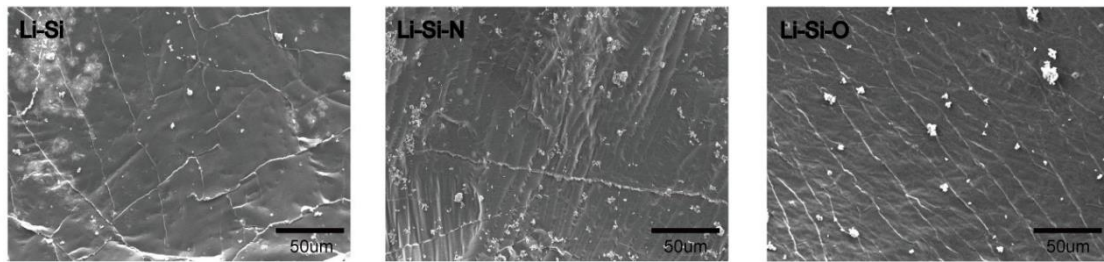


Figure 6. Scattering electron microscope (SEM) images of the electrode's surfaces after modification.

We were able to see that before the thermal treatment, whichever particles that are treated to the surface can be observed even with the naked eye. After heating, the particles of the initial silicon or silicon-functional group disappear, and the color of the anode surface changes significantly. Figure 6. shows the SEM image of the surface of the fabricated electrodes. Scratching the surface reveals unreacted lithium metal below the colored layer indicating that the reaction of lithium metal and silicon-functional group particles occurs on the surface and does not proceed within the inner parts of the electrode.

### **Electrochemical measurements.**

In order to compare the cycle lifetime and overpotentials of the modified electrodes, symmetric 2032 coin cells were employed. 1.3M LiPF<sub>6</sub> in ethyl carbonate/diethyl carbonate (3:7 vol%) with 10% fluoroethylene carbonate additive was used as an electrolyte. A polyethylene separator (Celgard 2325, 25μm) was used to prevent the electronic current between cathode and anode. Full cells were fabricated for further electrochemical performance evaluation. For full cell configuration, the modified lithium metal electrodes were used as the anode and LiNi<sub>0.6</sub>Co<sub>0.2</sub>Mn<sub>0.2</sub>O<sub>2</sub> (NCM622) was used as the cathode. The electrode composition of NCM622 cathode was the active materials of NCM622, super P, and PVDF binder with a 94 : 3 : 3 weight ratio, respectively. The same electrolyte and separator used in the symmetric cells were also used for the full cell tests.

### **Characterization**

Surface characterization was measured by SEM and XPS. SEM observation was conducted using a S-4800 field emission scanning electron microscope (Hitachi) at an acceleration voltage of 10.0kV to characterize the morphology of the modified electrode and the post-mortem analysis. For the XPS analysis, a K-Alpha X-ray Photoelectron Spectrometer (XPS) System (made by ThermoFisher Scientific) was used. A survey and depth profiles were taken to analyze the chemical composition with the different in-depth analysis. Depth profiles were measured with an etching for 0, 10, 300, and 600s.

### **Operando side-view optical microscopy observation**

For the operando side-view optical microscopy observation, a BX53MTRF-S model from Olympus was employed. Symmetric cells were fabricated using an ECC-Opto-SBS electrochemical test cell (EC-CELL) in an argon-filled glove box, composed of two lithium metal electrodes, and a glass-fiber filter separator (GFF, EC-CELL, 600μm). 1M LiPF<sub>6</sub> in EC/DEC (3:7 vol%) with 10% FEC additive was used as the electrolyte. The side-view of the fabricated symmetrical cell was observed through a Sapphire window, during galvanostatic performance evaluation by a BioLogic SP-200 battery tester. Lithium plating ( $\text{Li}^+ + \text{e}^- \rightarrow \text{Li}$ ) was conducted at a current density of 1mA/cm<sup>2</sup> for 10 hours. The cycling of the cell was done at a current density and plating/stripping capacity condition of 1mA/cm<sup>2</sup> and 2mAh/cm<sup>2</sup>, respectively.

## 2.2 Results and Discussion

### Surface characterization through XPS analysis

For surface and SEI layer characterization, XPS survey and depth profile was conducted to reveal the chemical composition of the electrode's surface and near-surface layer. A pristine electrode and an electrode that has been cycled once so that it can form the solid electrolyte interphase are analyzed. Pristine electrodes were analyzed only on the surface to reveal the chemical composition of the surface of the electrode. In-depth analysis was conducted for the cycled electrode to investigate the structure of the SEI layer formed.

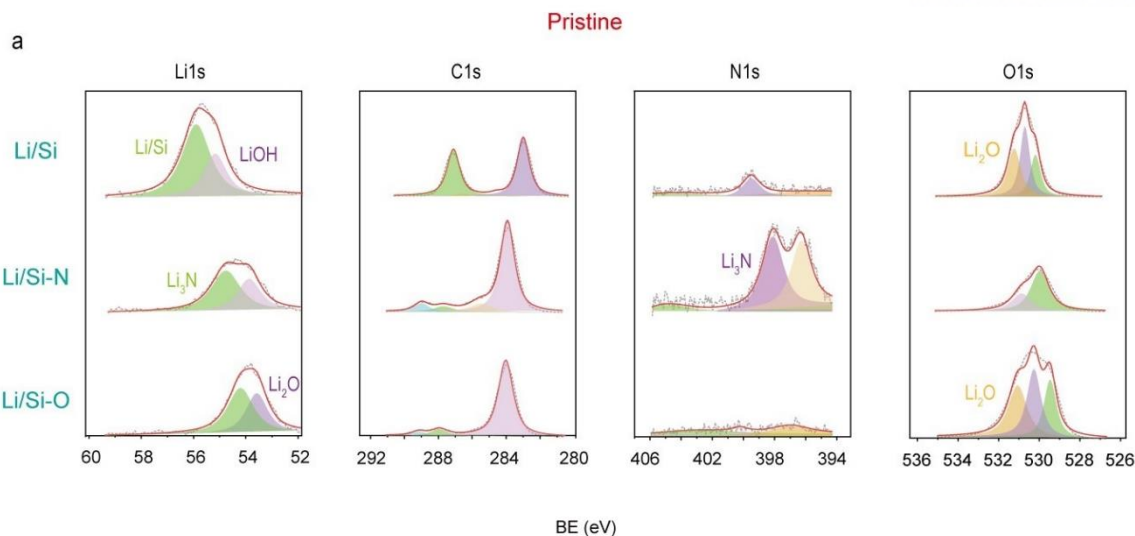


Figure 7. X-ray photoelectron spectroscopy (XPS) spectrum of each electrode right after their modifications.

Figure 7. shows the XPS spectrums of each modified electrode right after their fabrication. The silicon modified electrode's Li1s peaks show the prominent Li/Si alloy peak at 55.2 eV. It also shows a peak at 54.5 eV which is the LiOH component of the surface of the electrode, possibly formed due to exposure to air outside of the glove box. From the Li/Si-N electrodes we can observe a peak around 54.7eV which shows the existence of lithium nitride<sup>24</sup>. Li/Si-O modified electrodes show peaks from both Li<sub>2</sub>O (53.6eV) and Li/Si (54.7eV)<sup>24</sup>. The N1s peaks of both Li/Si and Li/Si-O modified electrodes does show a certain spectrum, but the overall lack of intensity compared to the other peaks (less than 3% of the intensities from Li1s, C1s, O1s peaks) shows that they are not a major component of the lithium metal electrode surface most likely resulting from side reactions or exposure to atmosphere. However, the N1s spectrum of the Li/Si-N anode shows much stronger and prominent peaks compared to its counterparts. The peak at 395.5eV shows the formation of Li<sub>3</sub>N at the surface of the electrode<sup>24</sup>. The additional peak located at 397.5eV originates from silicon nitride (Si<sub>3</sub>N<sub>4</sub>), which is from the remaining particles from the surface modification.

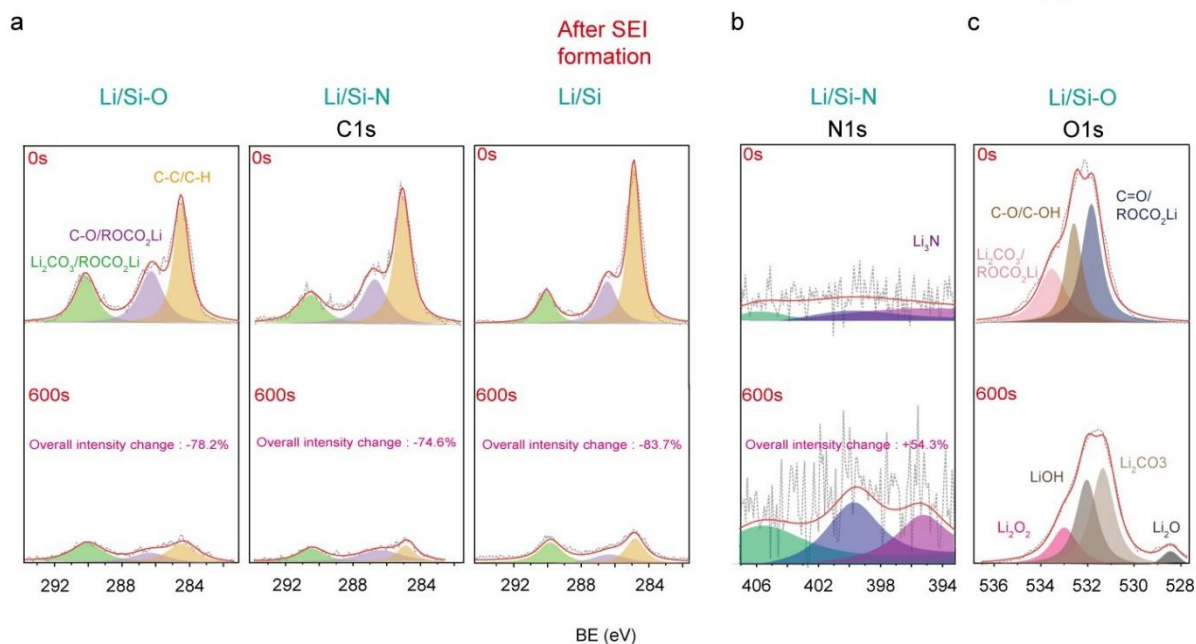


Figure 8. XPS depth profiling of the surfaces of each electrode after SEI layer formation.

Figure 8. shows the depth profiling results of the modified electrodes after allowing the SEI layer to form (1 cycle at  $0.1\text{ mA/cm}^2$  &  $1\text{ mAh/cm}^2$ ). The first most notable fact is the drastic decrease in intensity upon deeper profiles from the C1s peaks. The  $\text{ROCO}_2\text{Li}$ ,  $\text{Li}_2\text{CO}_3$ , C-O and C-H peaks that are located at 289.5, 286.5, and 284.6 eV respectively are mostly contributed from the organic components of the SEI layer that originate from the decomposition of the carbonate electrolyte<sup>25</sup>. The overall drop in intensity as XPS is measured deeper within the SEI layer means that most of the outer side of the SEI formed consists of organic components. Within the inner parts of the SEI layer lies the inorganic structure, which is also where the functional groups we used for surface modification exists. This can be seen from the N1s depth analysis results of the Li/Si-N modified electrode as well which shows a considerable amount of increase in intensity (54.3% increase) when measured deeper into the SEI layer. In particular, the  $\text{Li}_3\text{N}$  peak at 395.5 eV increases showing that the lithium nitride inorganic layer is lied well beneath the surface of the electrode. The XPS results of the Si-O modified electrode shows that O1s peaks originating from organic species ( $\text{ROCO}_2\text{Li}$ ) can be found in the outer surface of the SEI layer<sup>25</sup>. After 600s of etching, a slight shift in the peaks occurs. The shifted peaks originate from the inorganic ( $\text{Li}_2\text{O}_2$ ,  $\text{LiO}_2$ ,  $\text{LiOH}$ ,  $\text{Li}_2\text{CO}_3$ ) species showing that the inorganic layer and functional groups lie beneath the organic sheet.

### **Symmetrical cell performance evaluation.**

Electrochemical performance evaluation of symmetrical and full cells was conducted using coin cells. Symmetrical cells were put together using the surface modified electrodes (Si, SiO<sub>2</sub>, Si<sub>3</sub>N<sub>4</sub>) respectively. Each cell was tested at a current density and plating/stripping capacity condition of 1mA/cm<sup>2</sup>\_1mAh/cm<sup>2</sup>. Current tests were also conducted to evaluate the stability and reversibility of the electrodes. Current tests were conducted by running the cells for 10 cycles of changing current densities in the order of 1mA/cm<sup>2</sup>, 3mA/cm<sup>2</sup>, 5mA/cm<sup>2</sup>, and back to 1mA/cm<sup>2</sup>.

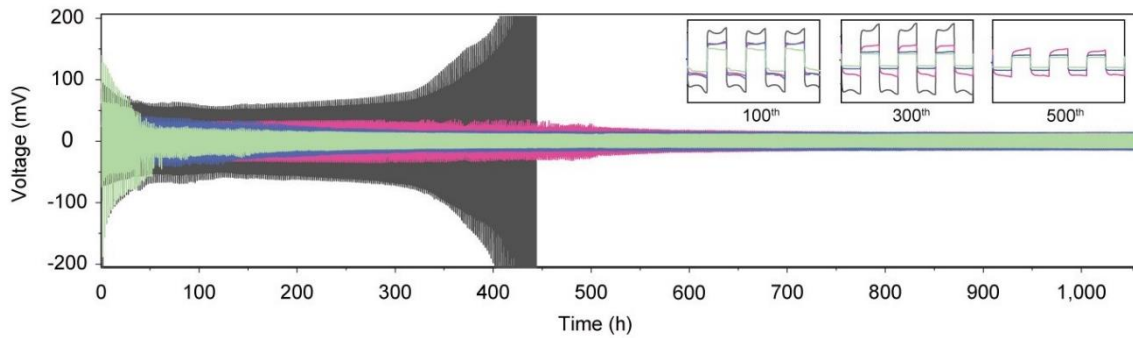


Figure 9. Cycling tests of symmetrical cells using modified lithium metal anodes vs a bare lithium metal anode.

Figure 9. shows the electrochemical performance of modified electrodes compared to bare lithium metal anodes at a current density of  $1\text{mA}/\text{cm}^2$ . All 3 modified electrodes showed significantly higher performances at a current density of  $1\text{mA}/\text{cm}^2$ . Each cell cycled for at least 1000 hours and was able to maintain a stable overpotential during that period. On the other hand, bare lithium showed a much higher overpotential throughout the cycling process which started to dramatically increase after the 175<sup>th</sup> cycle and was ultimately terminated around 450 hours of cycling. When looking into the specific overpotential of each electrode, it can be observed that the Si-N modified electrode maintains the lowest overpotential of 11.5mV as we have expected from the N-functionalized surface <sup>26</sup>.

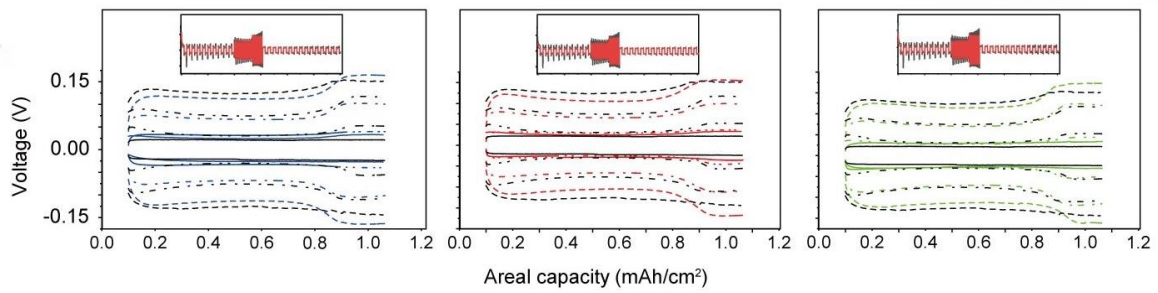


Figure 10. Overpotential profiles for current tests running in 10 cycles each at changing current densities from  $1 \text{ mA/cm}^2$ ,  $3 \text{ mA/cm}^2$ ,  $5 \text{ mA/cm}^2$ , and back to  $1 \text{ mA/cm}^2$ .

Figure 10. are the overpotentials from the current test results that shows all 3 modified electrodes have an overall lower overpotential compared to the bare lithium metal anode throughout the current test. The overpotential shown is the average overpotential of 10 cycles of each modified electrode cell at changing current densities ( $1, 3, 5 \text{ mA/cm}^2$ ). It is clear that the modification of the surface of the electrodes results in a lower overpotential thus showing improved stability and reversibility.



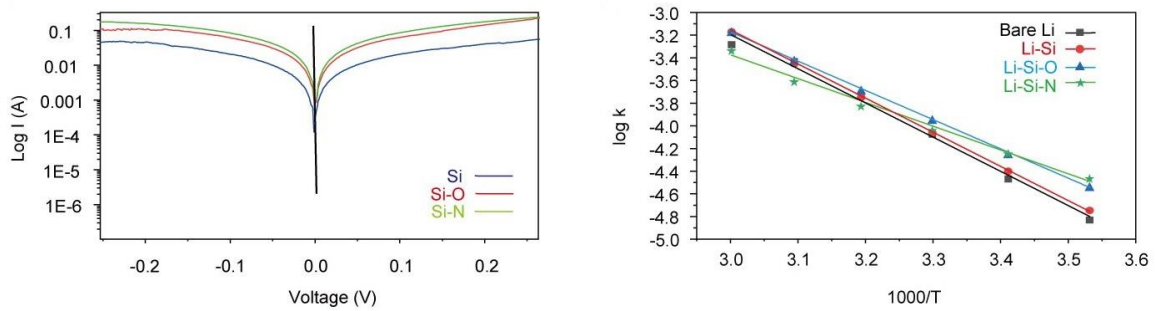


Figure 11. Tafel plots (left) and activation energies (right) of the modified electrodes.

Figure 11. shows the Tafel plot and activation energies of the Si, Si-O, Si-N modified electrode respectively converted from LSV evaluation and EIS results. Tafel plots show that the Si-N modified electrode shows the highest exchange current values indicating that the surface of the Si-N modified electrode has superior charge transfer properties compared to the other two electrodes.

Activation energies were calculated using ionic conductivity values that were derived resistance values obtained from EIS test results. Upon plotting the data, the Si-N modified electrode shows the lowest activation energy at approximately 0.417 eV. Bare lithium and Si modified electrodes show little difference in activation energy (0.599 eV, 0.598 eV respectively), however Si-O modified electrodes have a considerably lower 0.512 eV activation energy. This points out that the functional groups of the modified surface do affect the plating of lithium to some degree.

### Full cell performance evaluation

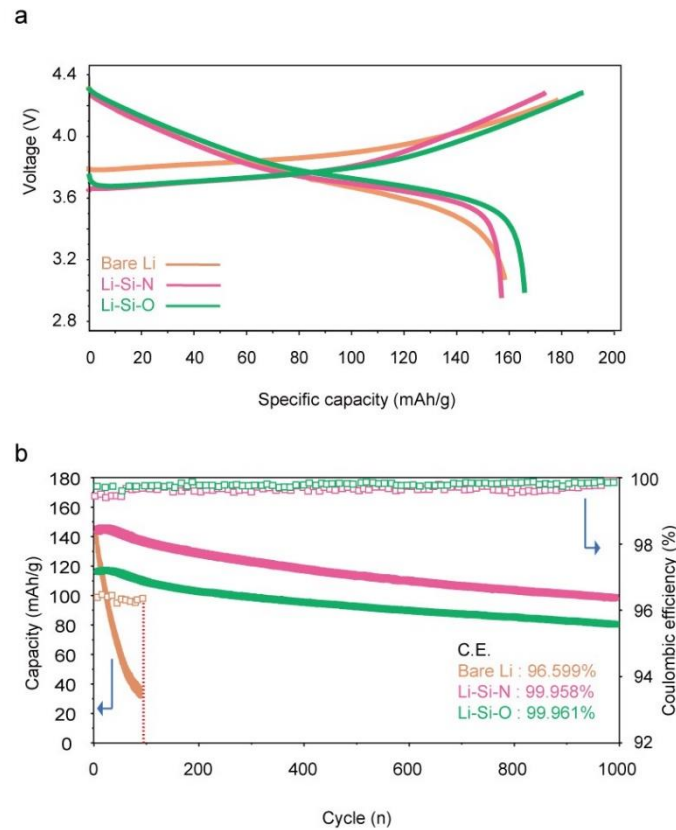


Figure 12. Full cell electrochemical performance. a) Initial capacity shown through a formation cycle. b) Cycle retention and coulombic efficiency (CE) of full cells using modified lithium metal anodes and NCM622 cathode.

Figure 12. shows the electrochemical performance of full cells. When compared to bare lithium cells the full cells show significantly increased cyclability and coulombic efficiency. The bare lithium full cell's capacity drops nearly 50% only after 50 cycles at a C-rate of 0.1C. On the other hand, both silica and silicon-nitride modified electrode full cells are able to maintain over 95% of their original capacity for the same number of cycles. Furthermore, at its 98<sup>th</sup> cycle the bare lithium cell reached just 31.65% of its original capacity and was terminated. On the other hand, both electrodes with modified surfaces ( $\text{Si}_3\text{N}_4$ ,  $\text{SiO}_2$ ) runs well over 700 cycles. At their 700<sup>th</sup> cycles they were able to maintain 72.47% (Si-N) and 74.11% (Si-O) of their original capacities. The coulombic efficiency of each sample shows a very high 99.954% (Si-N) and 99.957% (Si-O).

### Operando optical microscope (OM) observation

For further insight of the functionalities of the modified electrodes, optical microscopy was used. We observed the plating of lithium and cycling process (10 cycles) on the surface of each electrode. Inside a glove box with controlled Ar atmosphere, symmetric cells were constructed using an ECC-Opto-SBS electrochemical test cell (EC-CELL). The constructed cells were then electrochemically tested by Biologic SP-200 battery tester and observed from the side view through a Sapphire window.

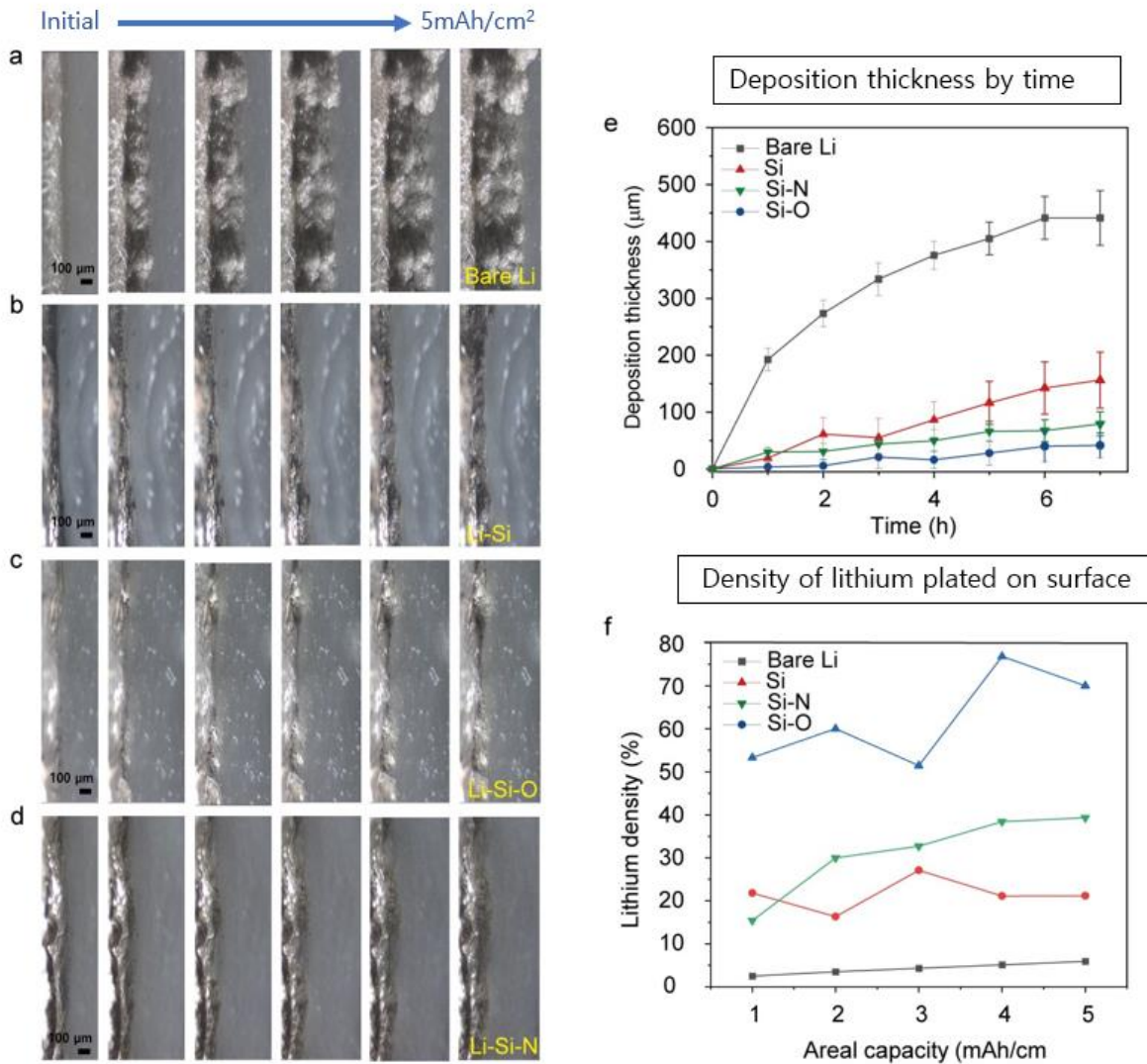


Figure 13. Lithium plating observed through operando OM observation. a-d. Lithium plating observed on the surface of each modified electrode. e. Lithium deposition thickness mapped by time and f. the density of the lithium plated throughout the surface of each electrode.

Figure 13 a-d. shows the lithium plating process ( $1\text{mA}/\text{cm}^2$ ,  $10\text{mAh}/\text{cm}^2$ ). Bare lithium (Fig 13a.) shows a dramatic amount of volume change when lithium metal is plated upon the surface of the

electrode. We were also able to observe an uneven distribution of the lithium-ion flux with lithium metal plating initialized on certain few points of the surface. The silicon modified electrode (Figure 13b.) shows a much smaller change in volume and a smoother surface compared to the bare lithium electrode. Not only does it show a more even surface, but we can also observe that the lithium metal seeds where the plating starts are more evenly distributed throughout the surface of the electrode. This shows that the lithium ionic flux can be improved to be more uniform when using Li-alloy metals, the main reason why we chose Si as the base material for our modification of LMA <sup>[10]</sup>. However, an even better morphology of the surface shows when we observe the lithium-alloy metal electrode with functional groups. The SiO<sub>2</sub> modified lithium metal anode (Figure 13c.) displays a minimal amount of volume change during plating whilst showing a relatively evenly spread lithium plating. Figure 13e. shows the thickness of plated lithium on each electrode as time flows. It is clearly indicated that the Si-O modified electrode shows the thinnest plating among the 4 electrodes followed closely by the Si-N modified electrode. The Si-N modified electrode (Figure 13d.) also shows a thin plating of lithium compared to the bare lithium and silicon modified electrodes.

Another point that is notable is the standard deviation of the plated lithium thickness. Although the silicon modified electrode shows a much thinner lithium plating, the deviation of the thickness along the surface of the electrode does not show much difference from the bare lithium metal anode. This shows that the lithium alloy metal helps keeping the volume change of the electrode down to a respective level, but it cannot produce an even surface on its own. On the other hand, when functional groups are added to the surface, it shows a thin plating and a low deviation of the plating thickness meaning that these additional features can contribute to a homogeneous lithium deposition.

We were also able to calculate the densities of plated lithium on each electrode from the obtained optical data. Figure 13f. shows the density of the lithium plated throughout the surface of the electrode. Lithium density can indicate the lithiophilicity and stability of the electrode's surface. Electrodes with modified surfaces show a significantly higher density compared to the electrode with a bare surface. Another noticeable point is that the silicon modified surface shows an overall lower density compared to silicon-functional group modified surfaces. This points to the fact that the functional groups, especially oxides can help to provide more dense and evenly plated surfaces.

## Conclusion

We were able to propose and manufacture a new lithium metal anode of which its surface is modified by using lithium alloy metal and its functional groups, hence without the help of electrolyte modification shows significantly enhanced performance compared to a bare lithium metal anode. Characterizing by SEM observation and XPS analysis we confirmed that depending on the functional group used the interphase layer consists of different components allowing the electrode to have different properties. Performance was evaluated by constructing both symmetric and full cells (NCM622) of each electrode. Modified electrodes showed much better performance in terms of cyclability, overpotential, and overall stability. Operando side-view optical microscopy observation also revealed the plating nature and surface properties of each electrode. By targeting the modification of the battery to the surface of the anode, no major changes to the electrolyte are necessary. This frees the cathode from any influence that may come from changing the electrolyte. The simple engineering process and confinement of the modification to the electrode surface can, hopefully, present a direction in which practical lithium metal anodes can be manufactured.

## References

- (1) Tarascon, J. M.; Armand, M. Issues and Challenges Facing Rechargeable Lithium Batteries. *Nature* **2001**, *414* (8), 359–367. <https://doi.org/10.1088/1751-8113/44/8/085201>.
- (2) Xu, W.; Wang, J.; Ding, F.; Chen, X.; Nasybulin, E.; Zhang, Y.; Zhang, J. G. Lithium Metal Anodes for Rechargeable Batteries. *Energy Environ. Sci.* **2014**, *7* (2), 513–537. <https://doi.org/10.1039/c3ee40795k>.
- (3) Fang, C.; Wang, X.; Meng, Y. S. Key Issues Hindering a Practical Lithium-Metal Anode. *Trends Chem.* **2019**, *1* (2), 152–158. <https://doi.org/10.1016/j.trechm.2019.02.015>.
- (4) Cheng, X. B.; Zhang, R.; Zhao, C. Z.; Zhang, Q. Toward Safe Lithium Metal Anode in Rechargeable Batteries: A Review. *Chem. Rev.* **2017**, *117* (15), 10403–10473. <https://doi.org/10.1021/acs.chemrev.7b00115>.
- (5) Lin, D.; Liu, Y.; Cui, Y. Reviving the Lithium Metal Anode for High-Energy Batteries. *Nat. Nanotechnol.* **2017**, *12* (3), 194–206. <https://doi.org/10.1038/nnano.2017.16>.
- (6) Dai, H.; Gu, X.; Dong, J.; Wang, C.; Lai, C.; Sun, S. Stabilizing Lithium Metal Anode by Octaphenyl Polyoxyethylene-Lithium Complexation. *Nat. Commun.* **2020**, *11* (1). <https://doi.org/10.1038/s41467-020-14505-8>.
- (7) Jang, E. K.; Ahn, J.; Yoon, S.; Cho, K. Y. High Dielectric, Robust Composite Protective Layer for Dendrite-Free and LiPF<sub>6</sub> Degradation-Free Lithium Metal Anode. *Adv. Funct. Mater.* **2019**, *29* (48), 1–9. <https://doi.org/10.1002/adfm.201905078>.
- (8) Zhao, C. Z.; Cheng, X. B.; Zhang, R.; Peng, H. J.; Huang, J. Q.; Ran, R.; Huang, Z. H.; Wei, F.; Zhang, Q. Li<sub>2</sub>S<sub>5</sub>-Based Ternary-Salt Electrolyte for Robust Lithium Metal Anode. *Energy Storage Mater.* **2016**, *3*, 77–84. <https://doi.org/10.1016/j.ensm.2016.01.007>.
- (9) Liu, F.; Wang, L.; Zhang, Z.; Shi, P.; Feng, Y.; Yao, Y.; Ye, S.; Wang, H.; Wu, X.; Yu, Y. A Mixed Lithium-Ion Conductive Li<sub>2</sub>S/Li<sub>2</sub>Se Protection Layer for Stable Lithium Metal Anode. *Adv. Funct. Mater.* **2020**, *30* (23), 1–9. <https://doi.org/10.1002/adfm.202001607>.
- (10) Kang, D.; Sardar, S.; Zhang, R.; Noam, H.; Chen, J.; Ma, L.; Liang, W.; Shi, C.; Lemmon, J. P. In-Situ Organic SEI Layer for Dendrite-Free Lithium Metal Anode. *Energy Storage Mater.* **2020**, *27* (January), 69–77. <https://doi.org/10.1016/j.ensm.2020.01.020>.
- (11) Schroder, K.; Alvarado, J.; Yersak, T. A.; Li, J.; Dudney, N.; Webb, L. J.; Meng, Y. S.; Stevenson, K. J. The Effect of Fluoroethylene Carbonate as an Additive on the Solid Electrolyte Interphase on Silicon Lithium-Ion Electrodes. *Chem. Mater.* **2015**, *27* (16), 5531–

5542. <https://doi.org/10.1021/acs.chemmater.5b01627>.
- (12) Cui, C.; Yang, C.; Eidson, N.; Chen, J.; Han, F.; Chen, L.; Luo, C.; Wang, P. F.; Fan, X.; Wang, C. A Highly Reversible, Dendrite-Free Lithium Metal Anode Enabled by a Lithium-Fluoride-Enriched Interphase. *Adv. Mater.* **2020**, *32* (12), 1–9. <https://doi.org/10.1002/adma.201906427>.
- (13) Boukamp, B. A.; Huggins, R. A. Lithium Ion Conductivity in Lithium Nitride. *Phys. Lett. A* **1976**, *58* (4), 231–233. [https://doi.org/10.1016/0375-9601\(76\)90082-7](https://doi.org/10.1016/0375-9601(76)90082-7).
- (14) Jin, H.; Liu, H.; Cheng, H.; Zhang, P.; Wang, M. The Synergistic Effect of Lithium Bis(Fluorosulfonyl)Imide and Lithium Nitrate for High-Performance Lithium Metal Anode. *J. Electroanal. Chem.* **2020**, *874*, 114484. <https://doi.org/10.1016/j.jelechem.2020.114484>.
- (15) Fu, J.; Ji, X.; Chen, J.; Chen, L.; Fan, X.; Mu, D.; Wang, C. Lithium Nitrate Regulated Sulfone Electrolytes for Lithium Metal Batteries. *Angew. Chemie* **2020**, *132* (49), 22378–22385. <https://doi.org/10.1002/ange.202009575>.
- (16) Yan, C.; Yao, Y. X.; Chen, X.; Cheng, X. B.; Zhang, X. Q.; Huang, J. Q.; Zhang, Q. Lithium Nitrate Solvation Chemistry in Carbonate Electrolyte Sustains High-Voltage Lithium Metal Batteries. *Angew. Chemie - Int. Ed.* **2018**, *57* (43), 14055–14059. <https://doi.org/10.1002/anie.201807034>.
- (17) Shin, H.; Park, J.; Sastry, A. M.; Lu, W. Effects of Fluoroethylene Carbonate (FEC) on Anode and Cathode Interfaces at Elevated Temperatures. *J. Electrochem. Soc.* **2015**, *162* (9), A1683–A1692. <https://doi.org/10.1149/2.0071509jes>.
- (18) Cabana, J.; Kwon, B. J.; Hu, L. Mechanisms of Degradation and Strategies for the Stabilization of Cathode-Electrolyte Interfaces in Li-Ion Batteries. *Acc. Chem. Res.* **2018**, *51* (2), 299–308. <https://doi.org/10.1021/acs.accounts.7b00482>.
- (19) Tang, W.; Yin, X.; Kang, S.; Chen, Z.; Tian, B.; Teo, S. L.; Wang, X.; Chi, X.; Loh, K. P.; Lee, H. W.; Zheng, G. W. Lithium Silicide Surface Enrichment: A Solution to Lithium Metal Battery. *Adv. Mater.* **2018**, *30* (34), 1–10. <https://doi.org/10.1002/adma.201801745>.
- (20) Chan, C. K.; Zhang, X. F.; Cui, Y. High Capacity Li Ion Battery Anodes Using Ge Nanowires. *Nano Lett.* **2008**, *8* (1), 307–309. <https://doi.org/10.1021/nl0727157>.
- (21) Ye, H.; Zheng, Z.; Yao, H.; Liu, S.; Zuo, T.; Wu, X.; Yin, Y.; Li, N.; Gu, J.; Cao, F.; Guo, Y. Guiding Uniform Li Plating/Stripping through Lithium–Aluminum Alloying Medium for Long-Life Li Metal Batteries. *Angew. Chemie* **2019**, *131* (4), 1106–1111. <https://doi.org/10.1002/ange.201811955>.



- (22) Kasavajjula, U.; Wang, C.; Appleby, A. J. Nano- and Bulk-Silicon-Based Insertion Anodes for Lithium-Ion Secondary Cells. *J. Power Sources* **2007**, *163* (2), 1003–1039. <https://doi.org/10.1016/j.jpowsour.2006.09.084>.
- (23) Go, W.; Kim, M. H.; Park, J.; Lim, C. H.; Joo, S. H.; Kim, Y.; Lee, H. W. Nanocrevasse-Rich Carbon Fibers for Stable Lithium and Sodium Metal Anodes. *Nano Lett.* **2019**, *19* (3), 1504–1511. <https://doi.org/10.1021/acs.nanolett.8b04106>.
- (24) Wood, K. N.; Teeter, G. XPS on Li-Battery-Related Compounds: Analysis of Inorganic SEI Phases and a Methodology for Charge Correction. *ACS Appl. Energy Mater.* **2018**, *1* (9), 4493–4504. <https://doi.org/10.1021/acsaem.8b00406>.
- (25) Wang, Z.; Qi, F.; Yin, L.; Shi, Y.; Sun, C.; An, B.; Cheng, H. M.; Li, F. An Anion-Tuned Solid Electrolyte Interphase with Fast Ion Transfer Kinetics for Stable Lithium Anodes. *Adv. Energy Mater.* **2020**, *10* (14), 1–9. <https://doi.org/10.1002/aenm.201903843>.
- (26) Alpen, U. v. Li<sub>3</sub>N: A Promising Li Ionic Conductor. *J. Solid State Chem.* **1979**, *29* (3), 379–392. [https://doi.org/10.1016/0022-4596\(79\)90195-6](https://doi.org/10.1016/0022-4596(79)90195-6).



## **Acknowledgements**

First, I would like to express gratitude to my advisor Prof. Hyun-Wook Lee who gave me the opportunity to continue my studies at the Ulsan National Institute of Science and Technology. Over the past 2 years he has been an excellent role model and an advisor in not only my studies but also in life. I will value deeply the education, advice and support that I have received during my Master's course.

I would also like to say that I am thankful to professors Youngsik Kim and Sung-Kyun Jung who have been supportive during the evaluation of my Master's defense. Although it was short term, I will always keep in mind the advice that both professors have given during my defense presentation.

I also thank my fellow ESEM lab members for their support throughout the past 2 years, especially Min-ho Kim and Juyoung Kim who have helped me in my research greatly.